Titanium-Doped Nickel Clusters TiNin (n=1-12): Geometry, Electronic, Magnetic, and Hydrogen Adsorption Properties

ARTICLE *in* THE JOURNAL OF PHYSICAL CHEMISTRY A · MARCH 2010

Impact Factor: 2.69 · DOI: 10.1021/jp100459c · Source: PubMed

4 AUTHORS, INCLUDING:

Venkataramanan Natarajan Sathiyamoorthy
SASTRA University
41 PUBLICATIONS **808** CITATIONS
SEE PROFILE

Yoshiyuki Kawazoe
Tohoku University
1,299 PUBLICATIONS **19,154** CITATIONS
SEE PROFILE

Titanium-Doped Nickel Clusters $TiNi_n$ ($n = 1-12$): Geometry, Electronic, Magnetic, and Hydrogen Adsorption Properties

Natarajan Sathiyamoorthy Venkataramanan,* Royoji Sahara, Hiroshi Mizuseki, and Yoshiyuki Kawazoe

Institute for Materials Research (IMR), 2-1-1, Katahira, Aoba-Ku, Sendai 980 8577, Japan

Received: January 17, 2010; Revised Manuscript Received: March 9, 2010

Using the first principles method, we study the growth behavior and electronic and magnetic properties of $TiNi_n$ ($n = 1-12$) clusters to clarify the effect of Ti modulation on the nickel nanostructures. Furthermore, chemisorption of H_2 was studied to understand the chemical reactivity of H_2 on the small Ni- and Ti-doped Ni clusters. The calculations are performed using the plane wave pseudopotential approach under the density functional theory and generalized gradient approximation for the exchange and correlation functional. The optimized geometries of $TiNi_{n-1}$ clusters indicate that the substitution of Ti brings a substantial structural reconstruction from 3D structure to a layer structure in which Ti atom is found to coordinate with Ni atoms to a maximum extent. This is accompanied by a significant enhancement in binding energies and reduction in chemical reactivity. Furthermore, the magnetic moments of the small Ti-doped Ni clusters are quenched because of the antiferromagnetic alignment of the Ti electrons. The lowest-energy structure of H_2 chemisorbed on Ni clusters shows that hydrogen prefers to adsorb on the edge site with two hydrogen atoms on these clusters in neighboring sites as the preferred arrangement. The incorporation of Ti atom improves the chemisorption energy of Ni clusters. Bader charge analysis indicates that with the formation of metal hydride, the H atoms withdraw charges from the metal centers, making them lose an electron, and carry a positive charge over them. Furthermore, Ti doping is found to enhance the chemical reactivity of Ni clusters.

I. Introduction

Over the past decade, a lot of emphasis has been paid to the study of the physical and chemical properties of atomic clusters, which are aggregates of atoms containing from a few to a few thousands atoms.[1,2] The studies on these clusters provide a unique opportunity to understand the evolution of cluster electronic structure from that of atoms in the bulk and also to study the physicochemical properties as a function of cluster size. The discovery of clusters with enhanced energetic stability, formed by a "magic" number of atoms, is one of the goals of cluster science because those interesting units can be used to assemble more complex materials further.[3] Extensive theoretical calculations have been conducted to examine structure, energetics, and stability of small clusters and to explore the potential to assemble crystals from them.[4,5]

Bimetallic transition metal (TM) clusters have attracted considerable attention in the past few years because of their novel optical properties, catalytic activity, and magnetic behavior.[6−8] The interaction between the two components in bimetallic clusters introduces a mutual influence on neighboring atoms and leads to the unique properties reported for these nanoalloys. Of particular interest was nickel−titanium bimetallic clusters because of their unique mechanical properties associated with reversible martensitic transformation.[9] Henceforth, the alloy found a great application as a shape memory alloy (SMA) and is commercially called NiTinol.

In the past two decades, several attempts were made to understand the structure, stability, and magnetic properties of small Ni and Ti clusters.[10−19] Previous studies have shown that Ni and Ti clusters possess complicated electronic ground-state structures and with magnetic moments due to the present of d electrons.[20,21] This may be the reason why studies on bimetallic clusters on Ni and Ti are scarce when compared with the simple monometallic clusters. The fusion of the Ni and Ti elements into one nanostructure entity may perhaps retain the chemical and magnetic properties of the individual components. Although there have been many studies on the TM doped with Ni clusters in recent years, there are still unclear issues in the structural and physical properties of these clusters.[22−29]

There has been an intense interest in examining the hydrogen interaction properties of isolated metal nanoparticles because of their relevance in hydrogen storage and catalysis.[30−32] The work on hydrogen storage is based on the premise that metal nanoparticles with their large surface area would enable the easy dissociation and adsorption of hydrogen atoms on the molecules. In the past, experimental studies on the polymer-coated palladium nanoparticles show improved hydrogen chemisorption over the bulk catalyst,[33] whereas recent vibrational spectral studies of hydrogen on the small nickel clusters indicate that molecular adsorption can occur on selective cluster sizes.[34,35] However, the binding energy of hydrogen on the metal surfaces was higher than desired for their practical applications in onboard hydrogen storage applications.[36,37]

Because many of the properties of nanoparticles depend on the size and nature of the materials, significant changes in their adsorption on hydrogen can be brought out by chemical modification by doping with other element on the surface of the nanoparticle.[38] So far, only very limited works on the hydrogen adsorption of the bimetallic clusters were reported. However, the interstitial metal hydrides hold the promise for hydrogen storage by providing binding energy close to the desired value and can be operated at the room temperature.[39]

* Corresponding author. E-mail: ramanan@imr.edu.

10.1021/jp100459c
Published on Web 03/24/2010

TABLE 1: Comparison of Calculated (GGA- PW91) and Experimental Bond Lengths, *d* (in angstroms), Binding Energy Per Atom, E_b (in electronvolts), and Magnetic Moment *M* (in μB) for the Diatomic Molecules Ni_2, Ti_2, NiH, and TiH Dimer

	Ni_2		Ti_2		NiTi		NiH		TiH	
parameters	calcd	exptl	calcd	exptl	calcd	exptl	calcd	exptl	calcd	exptl
d (Å)	2.080	2.154[a]	1.926		2.043		1.456	1.454[b]	1.754	
E_b (eV)	1.15	1.03[c]	1.61	2.10 to 1.05	1.92		2.45	2.70	1.87	1.96
M	2.0		4.0		2.0		1.0		3.0	

[a] From ref 46. [b] From ref 48. [c] From ref 47.

The presence of a small percentage of titanium was found to increase both the dehydrogenation and rehydrogenation kinetics of complex metal hydrides; however, the exact mechanism of this process is still under investigation.[40,41] Therefore, it would be interesting to elucidate the growth behavior and the adsorption of hydrogen on the Ti-doped Ni clusters.

In this article, equilibrium geometries of pure Ni_n ($n = 2-13$) clusters were optimized first based on the previous calculation results. For Ti-doped Ni clusters (Ni_nTi), we performed an extensive search for the ground-state structures and study the growth behavior and electronic and magnetic properties up to $n = 12$. Furthermore, we have studied the hydrogen chemisoption on these clusters and have calculated the chemisorption energy for the hydrogen on Ni- and Ti-doped Ni clusters. The article is organized as follows. Section II briefly describes the theoretical methods used in this work. In Section III, we present the lowest-energy structures and some metastable isomers and discuss the growth behavior, stability, and chemisorption of H_2 on these clusters. Finally, the conclusions of this work are made Section IV.

II. Computational Methods

The calculations presented here are carried out using the density functional theory within the pseudopotential plane wave method. We have used projector augmented wave (PAW) method and generalized gradient approximation (GGA) given by Perdew and Wang (PW-91) as implemented in the VASP package.[42,43] The clusters were placed in a cubic supercell with an edge of 15 Å, and periodic boundary conditions were imposed. The cutoff energy for the plane wave was set to 274.6 eV. Because of the large supercell and cluster calculation, the Brillouin zone integration is carried out using only the Γ point. The structures were considered to be converged when the force on each ion was <0.01 eV/Å, with a convergence in the total energy of about $10^{-4}-10^{-6}$ eV. The stability of lowest-energy configuration and the isomers of a given clusters were checked by performing calculations with different spin states. These lowest-energy structures of the Ti-doped Ni system were further checked by the ab initio simulated annealing method to avoid them being trapped in local minima in the entire potential surfaces. The above approaches have been found to been proven powerful to identify the ground states of nanoclusters.[44,45] However, no one can be sure that the true global minima were obtained, and at least, the present work will be a good starting point for understanding the growth pattern of these clusters. To check the accuracy of our calculation, we have compared the calculated binding energy and bond length of Ni_2 and Ti_2 with experimental values (Table 1). The results indicate that the chosen method predicts the bonding length and binding energy for Ti_2 and Ni_2 and NiH and TiH dimers.[48,48]

III. Results and Discussion

In this article, equilibrium geometries of pure Ni_n ($n = 2-13$) clusters were optimized first on the basis of the previous calculation results. Because there exists no prior knowledge on the structures of these Ti-doped Ni bimetallic clusters, we have performed an extensive search to find the minimum energy structure in two ways: (i) by considering the possible structures reported in the previous papers[49−53] and (2) by placing a Ti atom at various adsorption or substitutional sites on the basis of optimized Ni_n geometries, that is, Ti-capped, Ti-substituted, and Ti-concaved patterns as well as an Ni-capped pattern, which leads to numerous stable isomers.

A. Structure of $TiNi_n$ clusters ($n = 1$ to 12). The lowest-energy structures and some metastable low-energy isomers for $TiNi_n$ ($n = 1$ to 12) clusters obtained from this work are presented in Figures 1 and 2. The first one (number) represents the number of Ni atoms in the cluster, and the second one (letter) ranks the isomer in the descending order of the binding energy. The difference in total energies of the isomers from the lowest-energy isomer is given below the structure for each size. The structures for the pure nickel clusters are also plotted in Figures 1 and 2, which agree well with previous ab initio calculations and experimental data.[54] The calculated binding energy per atom (E_b), magnetic moment (*M*), and other relevant data for the lowest-energy structures of $TiNi_n$ are listed in Table 2.

The optimized bond lengths of Ni_2, Ni−Ti, and Ti_2 are 2.08, 2.04, and 1.92 Å, respectively. The Bader charge analysis indicates that a charge transfer occurs from the Ti atom to the Ni center. The interaction of Ti with Ni_2 dimer forms an open triangle structure with 119.5° for the <Ni−Ti−Ni angle and with Ni−Ti bond length of 2.03 Å, whereas the isosceles triangle lies as a metastable isomer with 0.322 eV higher in energy than the ground state. The geometry of the Ti-doped tetramer cluster was found to be a planar rhombus, whereas the Ni_4 has the tetrahedron structure as the ground state, which agrees well with the previous calculated results[55−57] but differs appreciably from the LSDA calculated method, which predicts a distorted tetrahedron.[58] In the case of pentamer, the Ti-doped Ni cluster has a 3D trigonal bipyramidal structure with Ti at the center and bonding with all Ni atoms was found to be the ground state, whereas the square pyramid was just 0.096 eV higher in energy than the ground-state structure. The shortest Ni−Ti bond length was found to be 2.11 Å. The ground-state geometry of the pure Ni cluster was found to be trigonal bipyramidal structure; however, a square pyramid was proposed on the basis of the ionization potential value.[59] This contrast arises because of the use of a different calculation method or exchange correlation used.

For the hexamer, a square pyramid structure was found to be the stable geometry in which the Ti atom is directly bonded to the four Ni atoms. The trigonal bipyramid-capped structure with one Ni atom, in which Ti atom is directly bonded to five other Ni atoms, was found to be a metastable isomer with 0.016 eV higher in energy than the ground-state geometry. For the heptamer, the pentagonal bipyramidal structure was found to be the ground-state geometry, whereas the Ni-atom-capped square bipyramidal structure was 0.154 eV higher in energy.

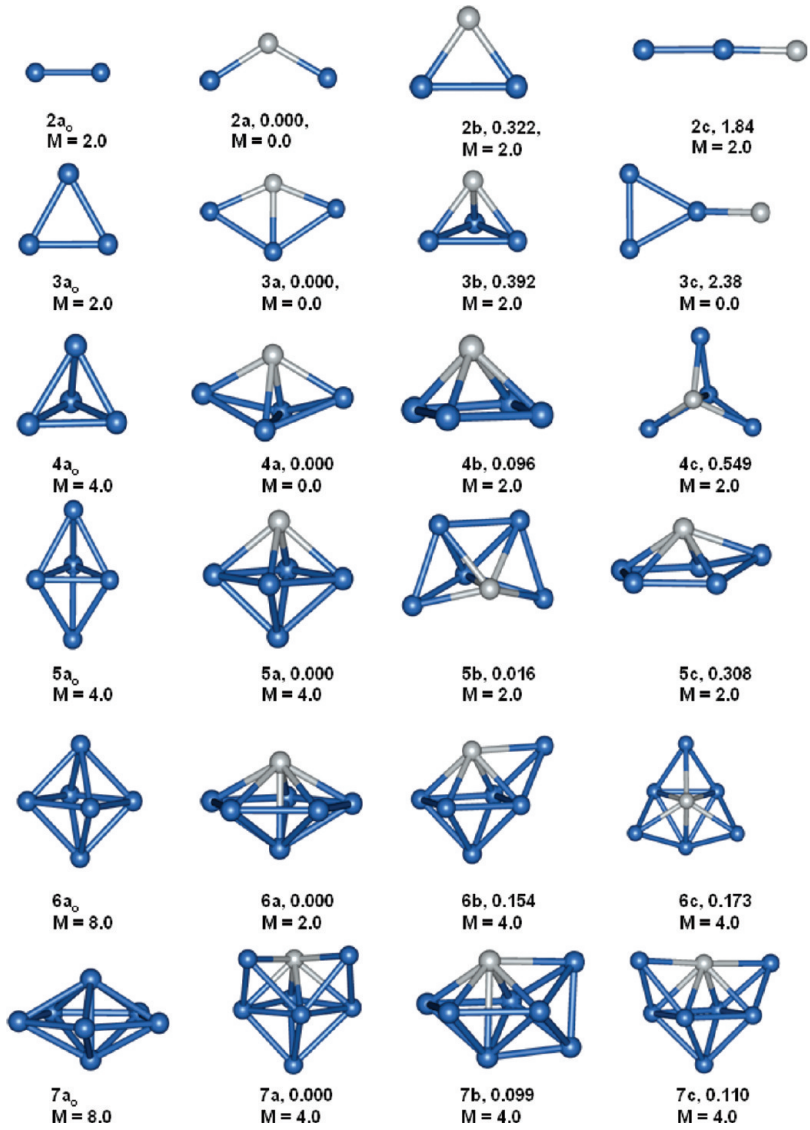

Figure 1. Lowest energy and low-lying structures of $TiNi_n$ ($n = 2-7$) clusters. The difference of total energies (electronvolts) of an isomer from the most favorable isomer are given below the structure for each size, and M is the total magnetic moment of the cluster.

The calculated shortest Ni−Ti bond length for the ground−state isomer was found to be 2.28 Å. For the octamer geometry, the bicapped square bipyramid structure was found to be the ground-state geometry, in which the Ti atoms were bonded to maximum Ni atoms, whereas the metastable isomer, where capped Ni atoms form a core, lies 0.099 eV higher in energy.

For the cluster size $n = 8$, the stable isomer is Ni-capped on the square bipyramidal structures where the Ti atoms bond seven Ni atoms. For the $n = 9$, a bicapped pentagonal bipyramidal structure was found to be ground-state geometry. For $n = 10-12$, the stable geometries were found to have a layer structure. These results show that the most stable geometry of the $TiNi_n$ clusters are formed, in which the Ti atom is found to coordinate with Ni atoms to a maximum extent. Compared with those of pure Ni_n clusters, there is substantial structural reconstruction after doping Ti atom. This change in structural transformation can be understood by the increased ionic radius of Ti atom compared with the Ni atom and because of the ability of Ti atoms to delocalize its 3d electrons, giving rise to empty antibonding d orbitals and facilitating close-packed structures.[60,61]

B. Energetics and Stability. In this section, we focus on the energetics and stability of the Ni- and Ti-doped Ni clusters. It is well known that the relative stability of the clusters can be predicted by calculating the binding energy per atom (E_b), second difference in energy (Δ_2E), and the dissociation energy (ΔE). E_b, Δ_2E, ΔE for the $TiNi_n$ clusters can be defined with the following formula

$$E_b = (E(\mathrm{Ti}) + nE(\mathrm{Ni}) - E(\mathrm{TiNi}_n))/(n+1) \quad (1)$$

$$\Delta_2E = E(\mathrm{TiNi}_{n-1}) + E(\mathrm{TiNi}_{n+1}) - 2E(\mathrm{TiNi}_n) \quad (2)$$

$$\Delta E = E(\mathrm{TiNi}_n) - (E(\mathrm{TiNi}_{n-1}) + E(\mathrm{Ti})) \quad (3)$$

where E(Ti), E(Ni), $E(\mathrm{TiNi}_n)$, $E(\mathrm{TiNi}_{n-1})$, and $E(\mathrm{TiNi}_{n+1})$ represent the total energies of the most stable Ti, Ni, TiNi*n*, $TiNi_{n-1}$, and $TiNi_{n+1}$ clusters, respectively.

The calculated E_b values are provided in Tables 1 and 2 and in Figure 3. The E_b of Ni_2, Ti_2, and Ni−Ti is 1.15, 1.61, and 1.92, respectively. The higher E_b for the bimetallic cluster reflects its higher stability. Figure 3 shows the E_b of Ni_n and $TiNi_{n-1}$ clusters as a function of the total number of atoms. The E_b values of the

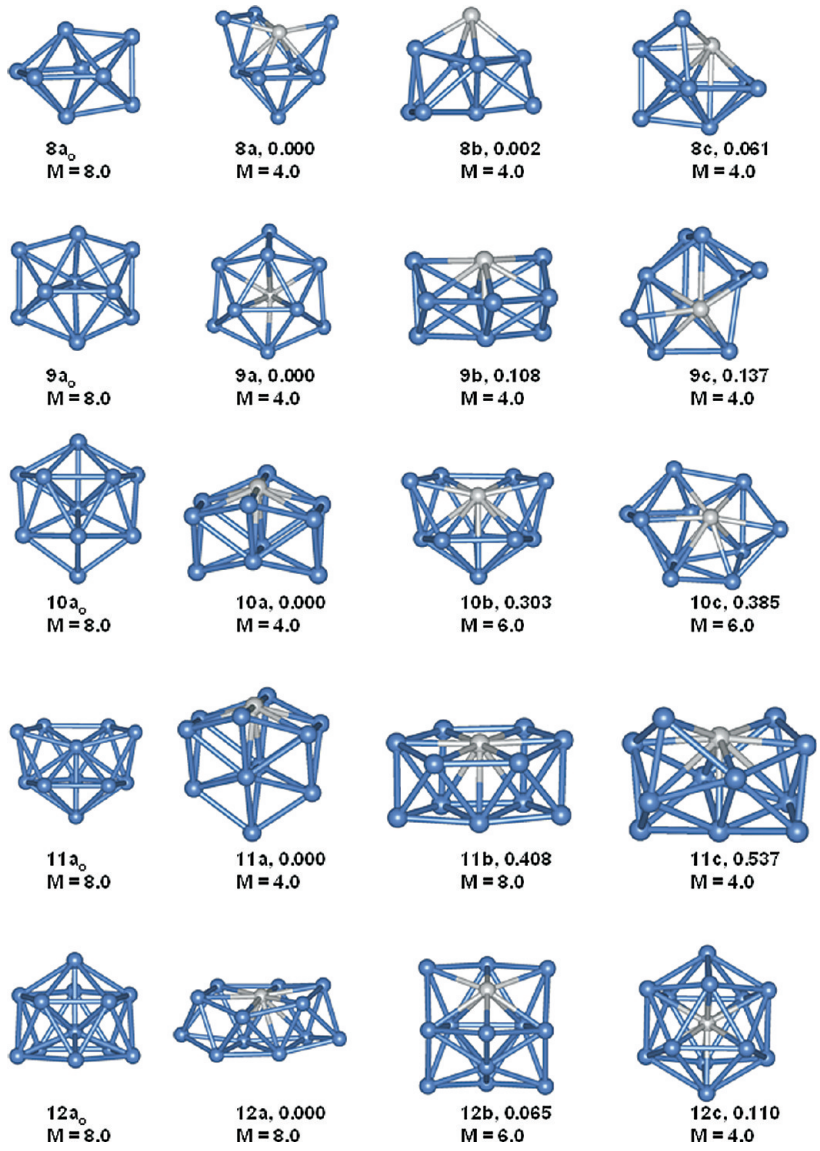

Figure 2. Lowest energy and low-lying structures of $TiNi_n$ ($n = 8-12$) clusters. The difference of total energies (electronvolts) of an isomer from the most favorable isomer are given below the structure for each size, and M is the total magnetic moment of the cluster.

TABLE 2: Calculated Binding Energy/Atom (E_b) Magnetic Moment on the Ti Atom, Total Magnetic Moment (M), Spin Gap (S_{gap}), and Atomic Bader Charge Ti Atoms for the Most Stable $TiNi_n$ Clusters

				S_{gap} (eV)	
$TiNi_n$ cluster n =	E_b (eV)	Bader charge on Ti (e)	total magnetic moment M (μB)	δ_1	δ_2
1	1.92	0.46	2.0	0.923	1.45
2	2.48	1.01	0.0	0.794	0.794
3	2.77	1.02	0.0	0.809	0.809
4	2.92	1.03	0.0	0.384	0.384
5	3.06	0.99	4.0	0.363	0.922
6	3.17	1.15	2.0	0.391	0.321
7	3.24	1.07	4.0	0.424	0.752
8	3.29	1.08	4.0	0.443	0.676
9	3.34	1.24	4.0	0.328	0.215
10	3.39	1.21	4.0	0.392	0.319
11	3.43	1.24	4.0	0.375	0.171
12	3.44	1.25	8.0	0.137	0.304

Ni_n and $TiNi_{n-1}$ clusters increase monotonically with the increase in atomic size and reach the bulk behavior. However, the incorporation of Ti atom improves the overall stability of the host Ni clusters. The higher stability of the $TiNi_{n-1}$ clusters is attributed to the higher bond strength of Ni−Ti than that of Ni−Ni, which are 1.92 and 1.15 eV, respectively. To know the clear insight into the relative stability of the $TiNi_{n-1}$ and Ni_n clusters, second-order difference in energy was calculated, and the results are shown in Figure 4. In the case of Ni_n clusters, an odd−even effect in the relative stability order were observed, whereas no such trend is

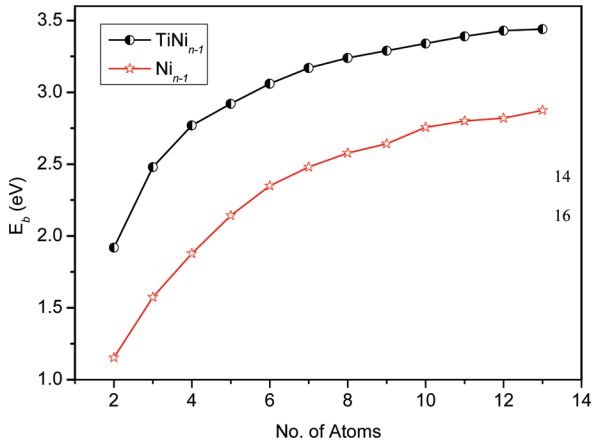

Figure 3. Calculated binding energy per atom of nickel clusters and Ti-doped Ni clusters ($n = 2-13$) plotted as a function of number of metal atoms.

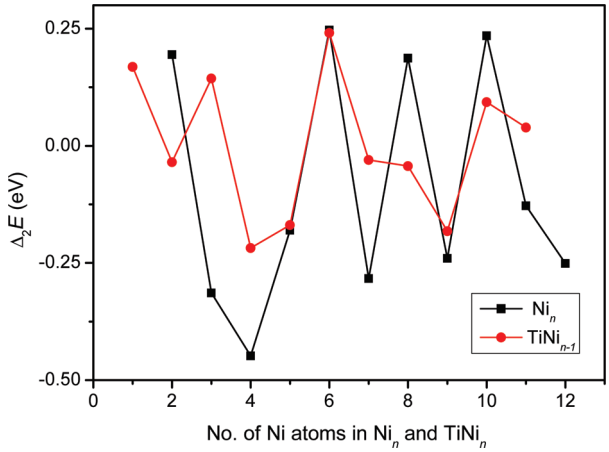

Figure 4. Calculated second difference in energies for the nickel clusters and Ti-doped Ni cluster as a function of number of Ni atoms.

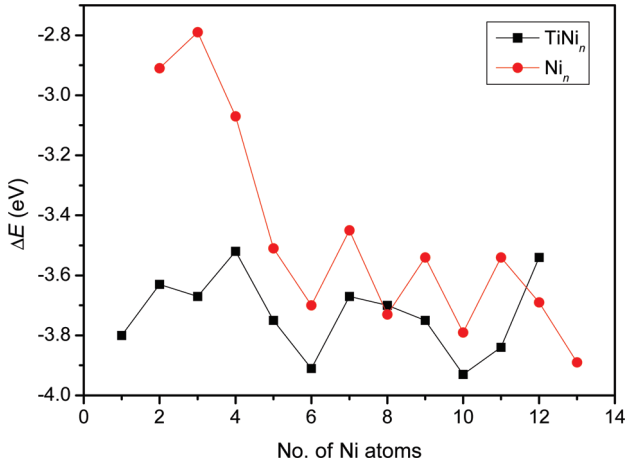

Figure 5. Calculated dissociation energy for the nickel clusters and Ti-doped Ni cluster as a function of number of Ni atoms.

seen in the Ti-doped Ni cluster. To get a clear understanding on the stability of the clusters, we calculated the dissociation energy of the Ni atom from the clusters using eq 3, and the obtained results are provided in the Figure 5. The pure Ni clusters show four dips at Ni_6, Ni_8, Ni_{10}, and Ni_{13}. On the contrary, Ti-doped Ni clusters show only three dips at $TiNi_3$, $TiNi_6$, and $TiNi_{10}$. Therefore, for

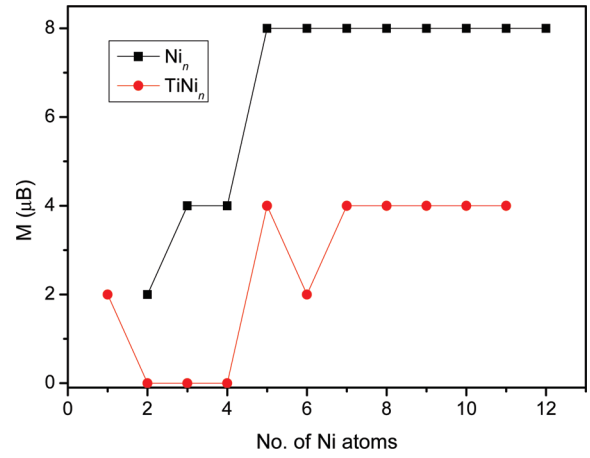

Figure 6. Calculated magnetic moment for the nickel clusters and Ti-doped Ni cluster as a function of number of Ni atoms.

the series of $TiNi_{n-1}$ clusters, the results suggest that $TiNi_3$, $TiNi_6$, and $TiNi_{10}$ were more stable as compared with their neighbors.

To verify the chemical stability of these clusters, we calculate the spin gap for the Ni_{n-1} and $TiNi_{n-1}$ clusters. Analogous to the HOMO−LUMO gap of a nonmagnetic cluster, one can define spin gaps for a magnetic cluster as

$$\delta_1 = -[\varepsilon_{\mathrm{HOMO}}^{\mathrm{majority}} - \varepsilon_{\mathrm{LUMO}}^{\mathrm{minority}}] \quad (4)$$

$$\delta_2 = -[\varepsilon_{\mathrm{HOMO}}^{\mathrm{majority}} - \varepsilon_{\mathrm{LUMO}}^{\mathrm{minority}}] \quad (5)$$

and the system is said to be stable if both δ_1 and δ_2 are positive.[62] In eqs 4 and 5, $\varepsilon_{\mathrm{HOMO}}^{\mathrm{majority}}$ is the HOMO level of the majority spin density, $\varepsilon_{\mathrm{LUMO}}^{\mathrm{minority}}$ is the LUMO level of the minority spin density, $\varepsilon_{\mathrm{HOMO}}^{\mathrm{minority}}$ is the HOMO level of minority spin density, and $\varepsilon_{\mathrm{LUMO}}^{\mathrm{majority}}$ is the LUMO level of minority spin density. The spin gaps represent the energy required to move an infinitesimal amount of charge from the HOMO of one spin channel to the LUMO of the other. Therefore, the magnitude of spin gaps is a measure of the chemical activeness of cluster. The spin gaps for $TiNi_{n-1}$ clusters are provided in Table 2, whereas those for the Ni_n are provided in the Supporting Information (Table S1). It is seen that both δ_1 and δ_2 are positive for all clusters. Furthermore, with the increase in cluster size, the δ_1 and δ_2 values were found to decreases. The higher spin gaps of the small size clusters are attributed to the quantum size effect. A comparison between the δ_1 and δ_2 values of large size Ni_n and $TiNi_{n-1}$ ($n > 8$) clusters shows that the spin gaps of pure Ni clusters are higher than the Ti-doped clusters, indicating that pure Ni clusters have higher activity compared with the doped clusters.

C. Magnetic Moment. Author: It is very important to investigate the magnetic properties of the TM clusters. The calculated magnetic moments for the pure Ni clusters are in agreement with previous findings;[54−57] however, some theoretical calculations predict higher magnetic moments for the small clusters.[58] This contrast arises because of the use of a different calculation method or exchange correlation. In Figure 6, we have plotted the magnetic moments of pure and Ti-doped Ni clusters at their stable geometries. It is seen from Figure 6 that magnetic moments of the dimer clusters are not quenched and are mainly located on the Ti atom. However, for the clusters with $n < 4$, the magnetic moments are completely quenched and are nonmagnetic. For the midsize clusters with $n > 7$, the

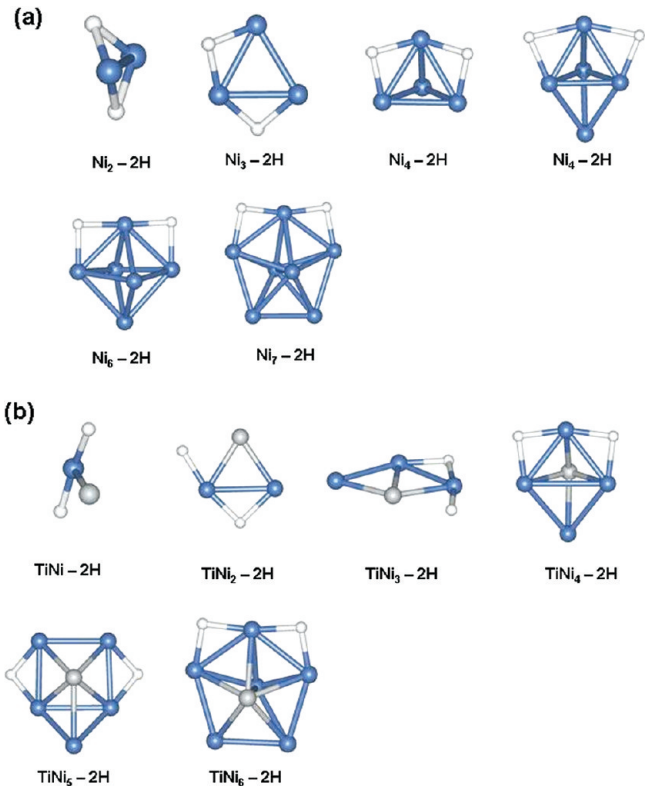

Figure 7. Lowest-energy structure of H_2 chemisorbed on (a) small Ni clusters and (b) Ti-doped Ni clusters.

magnetic moments are practically quenched with most of the local magnetic moments found to lie on the Ni atoms. To get clear insight, we made a Bader charge analysis for the lowest-energy structures. It is seen from Table 2, Bader charge analysis, that a weak charge transfer is found to occur in the case of dimer, whereas for the larger clusters, the amount of charge transfer from the Ti atom to the Ni center increases with the increase in clusters size. Furthermore, the magnetic moments of the Ti atom were found to align antiferromagnetically, whereas the local magnetic moment on Ni atoms was found to remain unaltered, even after doping the Ti atom[54]

D. Chemisorption of H_2 on $TiNi_n$ Clusters ($n = 1-7$). The main objective of the present study is to understand the chemical reactivity of H_2 on the small Ni- and Ti-doped Ni clusters. It is well known that H_2 will undergo a dissociative chemisorption on metal surfaces and clusters.[36,63−68] Therefore, we have performed a minimum energy structural search for the bare Ni_n- and Ti-doped Ni clusters $TiNi_{n-1}$ ($n = 7$). We have performed an extensive search to find the minimum energy structure by bringing H atoms from various directions and distances toward the lowest-energy structure and the first and second metastable structure of bare and Ti-doped Ni clusters. The lowest-energy structures with H_2 chemisorbed on bare Ni- and Ti-doped Ni clusters are shown in Figure 7. The lowest-energy structure of H_2 chemisorbed on Ni clusters shows that hydrogen prefers to adsorb on the edge site. Furthermore, the preferred arrangements of the two hydrogen atoms on these clusters were in two neighboring sites. However, a recent study on Pd clusters shows that the first hydrogen undergoes dissociative chemisorption on the faces of the clusters.[64] In general, the global minima of Ti-doped nickel clusters with two hydrogen atoms have the same nickel atom topology. The exception is the case of $TiNi_5$, where the lowest-energy structure was a square pyramidal structure

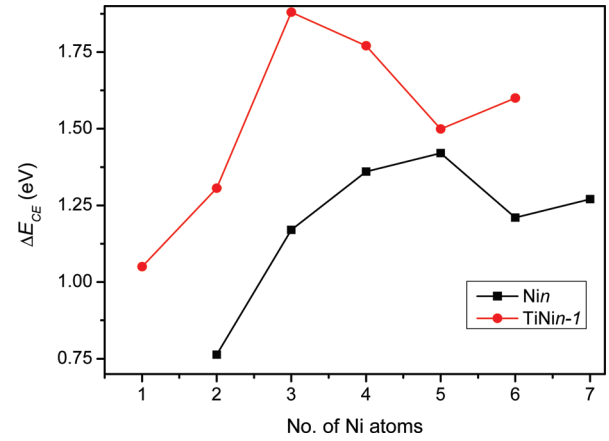

Figure 8. Chemisorption energy of hydrogen on nickel clusters and Ti-doped Ni cluster as a function of number of Ni atoms.

with Ni atom capped over it; however, the binding sites are analogues to the other Ti-doped Ni clusters.

The chemisorption energy, which is the energy to form the hydride species from $TiNi_n$ with H_2, was evaluated from the calculated energies of cluster with H_2 adsorbate using the equation

$$\Delta E_{CE} = E(TiNi_n) + E(H_2) - E(TiNi_n\text{-}H_2) \qquad (6)$$

where $E(TiNi_n)$ is the total energy of the lowest-energy structure of the Ti-doped Ni cluster, $E(H_2)$ is the total energy of the hydrogen molecule, and $E(TiNi_n\text{-}H_2)$ is the total energy of the hydride species formed on the Ti-doped Ni clusters.

The calculated chemisorption energies (ΔE_{CE}) corresponding to the most energetically favorable chemisorption site on the Ti-doped Ni cluster along with the chemisorption energy on H_2 on bare Ni clusters are shown in Figure 8 as a function of the cluster size. It is evident from Figure 8 that the chemisorption energy of H_2 on Ni_n and $TiNi_{n-1}$ clusters increases as a function of the total number Ni atoms. The ΔE_{CE} values of the Ni_n and $TiNi_{n-1}$ clusters have a similar trend in the values; however, the incorporation of Ti atom improves the chemisorption energy of the cluster. Among the clusters studies, Ni_5 and $TiNi_4$ clusters have higher chemisorption energy, whereas Ni_6 and $TiNi_5$ clusters have the least chemisorption energy. It will be worthwhile to specify that lanthanide (L)-doped Ni clusters with chemical composition LNi_5 were found to be good battery materials.[69] To understand the nature of interaction between the clusters and H_2, we have carried out the Bader charge analysis on the minimum energy clusters. Table 3 and Table S2 of the Supporting Information show the Bader charge on Ti and 2 H atoms for the Ti-doped system and the bare Ni clusters, respectively. As can be inferred from Table 3, with the formation of metal hydride, the H atoms withdraw charges from the metal centers, making them lose an electron, and carry a positive charges over them. The magnitude of charge transfer was found to decrease with the increase in cluster size and attain a constant value above the cluster size $n > 4$.

A comparison of charge transfer between bare H_2 chemisorbed Ni cluster and Ti-doped Ni clusters show that Ti doping facilitates the charge transfer from the metal atom to the H atoms. It is evident from this charge transfer that Ti doping enhances the chemisorption energy of Ni clusters. This effect may be used to alter the chemisorption properties of Ni nanostructures for hydrogen storage application. To confirm, we comparatively analyze the excess and depletion charge

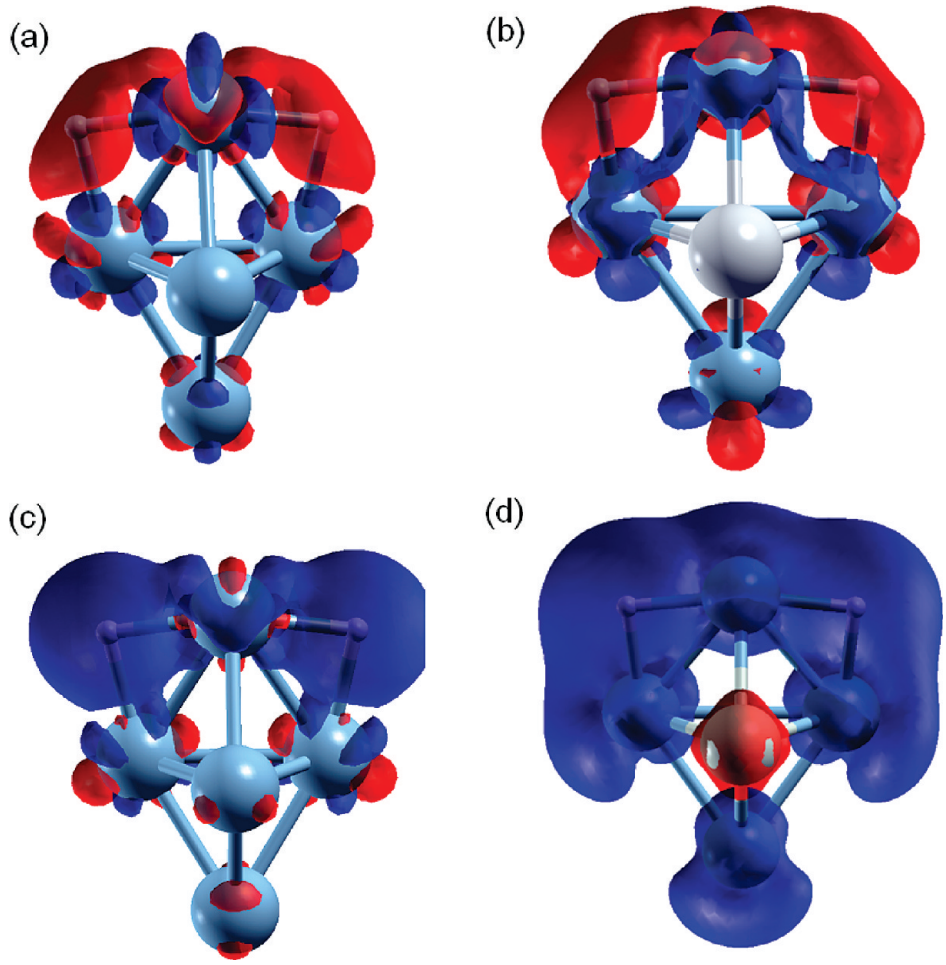

Figure 9. Plot of (a) charge density of H_2 chemisorbed Ni_5 and $TiNi_4$ cluster and (b) spin density of H_2 chemisorbed Ni_5 and $TiNi_4$ clusters.

TABLE 3: Calculated Chemisorption Energy/Atom (ΔE_{CE}), Spin Gap (S_{gap}), Magnetic Moment (M), and Atomic Bader Charge on Ti and H atoms for the Most Stable $TiNi_n$-H_2 Chemisorbed Clusters

		Bader charge (e)				S_{gap} (eV)	
$TiNi_n$-H_2 cluster n =	ΔE_{CE} (eV)	Ti	H1	H2	total magnetic moment M (μB)	δ_1	δ_2
1	1.05	0.682	−0.447	−0.353	2.0	1.05	1.55
2	1.31	0.827	−0.427	−0.357	0.0	0.631	0.631
3	1.88	1.11	−0.379	−0.444	0.0	1.06	1.06
4	1.77	1.02	−0.364	−0.355	0.0	0.666	0.666
5	1.50	1.09	−0.350	−0.346	2.0	0.406	0.934
6	1.61	1.13	−0.368	−0.365	2.0	0.239	0.407

density for the Ni hydride (Ni_5-2H) and the Ti-doped Ni hydride ($TiNi_4$-2H) systems. As seen in Figure 9a,b, the charges are depleted at the metal center and excesses on the hydrogen atom.

We then explored the magnetic moments on these clusters. The magnetic moments of the hydrogen chemisorbed $TiNi_n$ ($n \leq 8$) clusters have a similar trend as those of the bare $TiNi_n$; however, the magnitude of the clusters of $n = 5$ and 6 were partially quenched. To understand the quenching in magnetic moment, we calculate the spin density difference of the system, which is defined as the difference between the total spin density and the atomic spin densities for the Ni_5-2H and $TiNi_4$-2H systems. It is seen from Figure 9c,d, magnetic moments of Ti atoms were found to align antiferromagnetically, leading to the quenching in the magnetic moments of these clusters.

To understand the chemical stability, we calculated the S_{gap} for the Ti-doped Ni clusters at their stable geometry using eqs 3 and 4. A plot of S_{gap} between the bare $TiNi_n$ along with the hydrogen chemisorbed system is shown in the Supporting Information (Figure S1). In Figure S1, the chemical reactivity of H_2 chemisorbed clusters is higher than that for the pure Ti-doped Ni clusters. Therefore, Ti-doped Ni clusters would be a better catalyst for the hydrogenation reactions. To know the effect of Ti doping on the chemical stability of chemisorbed clusters, we have plotted the S_{gap} of H_2 chemisorbed on bare Ni- and Ti-doped Ni clusters (Figure S2, Supporting Information). As can be seen from Figure S2, the S_{gap} for the H_2 chemisorbed Ti-doped Ni clusters is higher than that of the bare Ni clusters. Consequently, Ti doping on Ni clusters would provide higher chemical reactivity during the hydrogenation reactions.

IV. Conclusions

A systematic theoretical study on the growth behavior and electronic and magnetic properties of $TiNi_n$ ($n = 12$) clusters has been performed to clarify the effect of Ti modulation on the nickel

nanostructures. The results show that Ti doping brings a substantial structural reconstruction from 3D structure to a layer structure in which Ti atom is found to coordinate with Ni atoms to a maximum extent because of the increased ionic radius of Ti atom and because of the ability of Ti atoms to delocalize their 3d electrons. This is accompanied by a significant enhancement in binding energies and reduction in chemical reactivity. Furthermore, the magnetic moments of the small Ti-doped Ni clusters are quenched because of the antiferromagnetic alignment of the Ti electrons.

The chemisorption of H_2 was studied to understand the chemical reactivity of H_2 on the small Ni- and Ti-doped Ni clusters. The lowest-energy structure of H_2 chemisorbed on Ni clusters shows that hydrogen prefers to adsorb on the edge site. Furthermore, the preferred arrangements of the two hydrogen atoms on these clusters were in two neighboring sites. In general, the global minima of Ti-doped nickel clusters with two hydrogen atoms have the same nickel atom topology. The chemisorption energy of the Ni_n and $TiNi_{n-1}$ clusters has a similar trend in the values; however the incorporation of the Ti atom improves the chemisorption energy of the cluster. Bader charge analysis indicates that with the formation of metal hydride, the H atoms withdraw charges from the metal centers, making them lose an electron, and carry a positive charge over them. Furthermore, Ti doping was found to enhance the chemical reactivity of Ni clusters. Therefore, our findings contribute to the selective design of hydrogen storage materials/hydrogenation catalyst.

Acknowledgment. We thank Dr. Vijaya Kumar and Dr. M. Saeed Bhramy for their helpful suggestion and useful discussion. This work has been supported by New Energy and Industrial Technology Development Organization (NEDO) under "Advanced Fundamental Research Project on Hydrogen Storage Materials. The authors thank the crew of the Center for Computational Materials Science at Institute for Materials Research, Tohoku University, for their continuous support of the HITACHI SR11000 supercomputing facility.

Supporting Information Available: Spin gap for the nickel cluster and Ti-doped cluster, hydrogen chemisorbed on nickel cluster and Ti-doped nickel clusters, calculated binding energy/atom, spin gap, magnetic moment for the sable nickel cluster and chemisorption energy, spin gap, magnetic moment, and Barder charge. This material is available free of charge via the Internet at http://pubs.acs.org.

References and Notes

(1) *Clusters and Nanomaterials: Theory and Experiment*; Kawazoe, Y., Kondow, T., Ohno, K., Eds.; Springer-Verlag: New York, 2002.
(2) Ferrando, R.; Jellinek, J.; Johnston, R. L. *Chem. Rev.* **2008**, *108*, 846.
(3) Alonso, J. A. *Chem. Rev.* **2000**, *100*, 637.
(4) *Nano-Scale Materials*; Sahu, S. N., Choudhury, R. K., Jena, P., Eds.; Nova Science Publishers: New York, 2004.
(5) *Physics and Chemistry of Finite Systems: From Clusters to Crystals*; Jena, P., Khanna, S. N., Rao, B. K., Eds.; Kluwer Academic: Dordrecht, The Netherlands, 1992.
(6) Alonso, J. A. *Bimetallic Clusters, Structure and Properties of Atomic Nanoclusters*; Imperial College Press: London, 2005.
(7) Mottet, C.; Rossi, G.; Balleto, F.; Ferrando, R. *Phys. Rev. Lett.* **2005**, *95*, 035501.
(8) Aguado, A.; Gonzalez, L. E.; Lopez, J. M. *J. Phys. Chem. B* **2004**, *108*, 11722.
(9) Huang, X.; Ackland, G. J.; Rabe, K. M. *Nat. Mater.* **2003**, *2*, 307.
(10) Nayak, S. K.; Khanna, S. N.; Rao, B. K.; Jena, P. *J. Phys. Chem. A* **1997**, *101*, 1072.
(11) Reddy, B. V.; Nayak, S. K.; Khanna, S. N.; Rao, B. K.; Jena, P. *J. Phys. Chem. A* **1998**, *102*, 1748.
(12) Parks, E. K.; Zhu, L.; Ho, J.; Riley, S. J. *J. Chem. Phys.* **1994**, *100*, 7206.
(13) Aguilera-Granja, F.; Bouarab, S.; Lopez, M. J.; Vega, A.; Montejano-Carrizales, J. M.; Iniguez, M. P.; Alonso, J. A. *Phys. Rev. B* **1998**, *57*, 12469.
(14) Estiu, G. L.; Zerner, M. C. *J. Phys. Chem.* **1996**, *100*, 16874.
(15) Arvizu, G. L.; Calaminici, P. *J. Chem. Phys.* **2007**, *126*, 194102.
(16) Petkov, S. P.; Vayssilov, G. N.; Kruger, S.; Rosch, N. *Chem. Phys.* **2008**, *348*, 61.
(17) Shang, M. H.; Wei, S. H.; Zhu, Y. J. *J. Phys. Chem. C* **2009**, *113*, 15507.
(18) Salazar-Villanueva, M.; Tejeda, P. H. H.; Pal, U.; Rivas-Silva, J. F.; Mora, J. I. R.; Ascenicio, J. A. *J. Phys. Chem. A* **2006**, *110*, 10274.
(19) Du, J. A.; Wang, H. Y.; Jiang, G. *J. Mol. Struct. THEOCHEM* **2007**, *817*, 47.
(20) Venkataramanan, N. S. *J. Mol. Struct. THEOCHEM* **2008**, *856*, 9.
(21) Liu, H. B.; Canizal, G.; Schabes-Retchkiman, P. S.; Ascencio, J. A. *J. Phys. Chem. B* **2006**, *110*, 12333.
(22) Kruger, S.; Stener, M.; Rosch, N. *J. Chem. Phys.* **2001**, *114*, 5207.
(23) Finetti, M.; Ottavianelli, E. E.; Diez, R. P.; Jubert, A. H. *Comput. Mater. Sci.* **2001**, *20*, 57.
(24) Deshpande, M. D.; Roy, S.; Kanhere, D. G. *Phys. Rev. B* **2007**, *76*, 195423.
(25) Dennler, S.; Chavez, J. L. R.; Morillo, J.; Pastor, G. M. *Eur. Phys. J. D* **2003**, *24*, 237.
(26) Harb, M.; Rabilloud, F.; Simon, D. *J. Phys. Chem. A* **2007**, *111*, 7726.
(27) Rexer, E. F.; Jellinek, J.; Krissinel, E. B.; Parks, E. K.; Riley, S. J. *J. Chem. Phys.* **2002**, *117*, 82.
(28) Feng, C. J.; Xue, Y. H.; Zhang, X. Y.; Zhang, X. C. *Chin. Phys. B* **2009**, *18*, 1436.
(29) Hristova, E.; Dong, Y.; Grigoryan, V. G.; Springborg, M. *J. Phys. Chem. A* **2008**, *112*, 7905.
(30) Knickelbein, M. B. *Annu. Rev. Phys. Chem.* **1999**, *50*, 79.
(31) Chen, B.; Gomez, M. A.; Doll, J. D.; Freeman, D. L. *J. Chem. Phys.* **1998**, *108*, 4031.
(32) Petkov, P.St.; Vayssilov, G. N.; Kruger, S.; Rosch, N. *J. Phys. Chem. A* **2008**, *112*, 8523.
(33) Nobuhara, K.; Nakanishi, H.; Kasai, H.; Okiji, A. *J. Appl. Phys.* **2000**, *88*, 6897.
(34) Swart, I.; de Groot, F. M. F.; Weckhuysen, B. M.; Gruene, P.; Meijer, G.; Filelicke, A. *J. Phys. Chem. A* **2008**, *112*, 1139.
(35) Swart, I.; Gruene, P.; Filelicke, A.; Meiger, G.; Weckhuysen, B. M.; de Groot, F. M. F. *Phys. Chem. Chem. Phys.* **2008**, *10*, 5743.
(36) Venkataramanan, N. S.; Khazaei, M.; Sahara, R.; Mizuseki, H.; Kawazoe, Y. *Chem. Phys.* **2009**, *359*, 173.
(37) Zhao, X. Y.; Ma, L. Q. *Int. J. Hydrogen Energy* **2009**, *34*, 4788.
(38) Tarakeshwar, P.; Kumar, T. J. D.; Balakrishnan, N. *J. Chem. Phys.* **2009**, *130*, 114301.
(39) Eberle, U.; Felderhoff, M.; Schuth, F. *Angew. Chem., Int. Ed.* **2009**, *48*, 6608.
(40) Bogdanovic, B.; Schwickardi, M. *J. Alloy. Compd.* **1997**, *253*, 1.
(41) Huang, C. K.; Zhao, Y. J.; Sun, T.; Guo, J.; Sun, L. X.; Zhu, M. *J. Phys. Chem. C* **2009**, *113*, 9936.
(42) Perdew, J. P.; Wang, Y. *Phys. Rev. B* **1992**, *45*, 13244.
(43) Kresse, G.; Joubert, D. *Phys. Rev. B* **1999**, *59*, 1758.
(44) Wu, J.; Hagelberg, F. *J. Phys. Chem. A* **2006**, *110*, 5901.
(45) Li, S. F.; Shao, Z.; Han, S.; Xue, X.; Wang, F.; Sun, Q.; Jia, Y.; Guo, Z. X. *J. Chem. Phys.* **2009**, *131*, 184301.
(46) Pinegar, J. C.; Langenberg, J. D.; Arrington, C. A.; Spain, E. M.; Morese, M. D. *J. Chem. Phys.* **1995**, *102*, 666.
(47) Morse, M. D.; Hansen, G. P.; Langridge-Smith, P. R. R.; Zheng, L.-S.; Geusic, M. E.; Michalopoulos, D. L.; Smalley, R. E. *J. Chem. Phys.* **1980**, *80*, 5400.
(48) Curotto, E.; Matro, A.; Freeman, D. L.; Doll, J. D. *J. Chem. Phys.* **1998**, *108*, 729.
(49) Harb, M.; Rabilloud, F.; Simon, D. *J. Chem. Phys.* **2009**, *131*, 174302.
(50) Rajesh, C.; Majumder, C. *J. Chem. Phys.* **2009**, *130*, 234309.
(51) Bakken, V.; Swang, O. *J. Chem. Phys.* **2008**, *128*, 084712.
(52) Cerowski, V.; Rao, B. K.; Khanna, S. N.; Jena, P.; Ishii, S.; Ohno, K.; Kawazoe, Y. *J. Chem. Phys.* **2005**, *123*, 074329.
(53) Pittaway, F.; Paz-Borbon, L. O.; Johnston, R. L.; Arslan, H.; Ferrando, R.; Mottet, C.; Barcaro, G.; Fortunelli, A. *J. Chem. Phys. C* **2009**, *113*, 9141.
(54) Futschek, T.; Hafner, J.; Marsman, M. *J. Phys.: Condens. Matter* **2006**, *18*, 9703.
(55) Cisneros, G. A.; Castro, M.; Salahub, D. R. *Int. J. Quantum Chem.* **1999**, *75*, 847.
(56) Castro, M.; Jamorski, C.; Salahub, D. R. *Chem. Phys. Lett.* **1997**, *271*, 133.
(57) Michelini, M. C.; Diez, R. P.; Jubert, A. H. *J. Mol. Struct. THEOCHEM* **1999**, *490*, 181.
(58) Reuse, F. A.; Khanna, S. N. *Chem. Phys. Lett.* **1995**, *234*, 77.
(59) Michelini, M. C.; Diez, R. P.; Jubert, A. H. *Comput. Mater. Sci.* **2004**, *31*, 292.
(60) Du, J. G.; Sun, X. Y.; Jiang, G. *Eur. Phys. J. D* **2009**, *55*, 111.
(61) Ma, L.; Zhao, J.; Wang, J.; Wang, B.; Lu, Q.; Wang, G. *Phys. Rev. B* **2006**, *73*, 125439.

(62) Datta, S.; Kabir, M.; Saha-Dasgupta, T.; Mookerjee, A. *Phys. Rev. B* **2009**, *80*, 085418.
(63) Tarakeshwar, P.; Kumar, T. J. D.; Balakrishnan, N. *J. Phys. Chem. A* **2008**, *112*, 2846.
(64) Zhou, C.; Yao, S.; Wu, J.; Forrey, R. C.; Chen, L.; Tachibana, A.; Cheng, H. *Phys. Chem. Chem. Phys.* **2008**, *10*, 5445.
(65) Henry, D. J.; Varano, A.; Yarovsky, I. *J. Phys. Chem. A* **2009**, *113*, 5832.
(66) Yang, H.; Whitten, J. L. *J. Chem. Phys.* **1993**, *98*, 5039.
(67) Petkov, P. S.; Vayssilov, G. N.; Kruger, S.; Rosch, N. *Chem. Phys.* **2008**, *348*, 61.
(68) Liu, B.; Lusk, M. T.; Ely, J. F. *J. Phys. Chem. C* **2009**, *113*, 13715.
(69) Jiang, W. Q.; Lan, Z. Q.; Xu, L. Q.; Lia, G. X.; Guo, J. *Int. J. Hydrogen Energy* **2009**, *34*, 4827.

JP100459C